INTERNATIONAL ATOMIC ENERGY AGENCY
UNITED NATIONS EDUCATIONAL, SCIENTIFIC AND CULTURAL ORGANIZATION

INTERNATIONAL CENTRE FOR THEORETICAL PHYSICS
34100 TRIESTE (ITALY) - P.O.B. 586 - MIRAMARE - STRADA COSTIERA 11 - TELEPHONES: 224281/2/3/4/5/6
CABLE: CENTRATOM - TELEX 460392-1

SMR/100 - 47

WINTER COLLEGE ON LASERS, ATOMIC AND MOLECULAR PHYSICS

(24 January - 25 March 1983)

Coherent Transient Phenomena Experiments

H.M. GIBBS

Optical Sciences Center
University of Arizona
Tucson, Arizona 85721
U.S.A.

References for the lectures on "Coherent Transient Phenomena Experiments," by Hyatt M. Gibbs scheduled for March 9 and 10.

I. THIN-SAMPLE EXPERIMENTS (effect of atoms on field can be neglected)

A. Resonance Fluorescence (RF)

1. Observation of narrower than natural linewidth fluorescence with weak coherent field:

RF1. H. M. Gibbs and T. N. C. Venkatesan, Opt. Commun. 17, 87 (1976).

2. Resonance fluorescence triplet with strong coherent field:

RF2. F. Y. Wu, R. E. Grove, and S. Ezekiel, Phys. Rev. Lett. 35 1426 (1975).

RF3. W. Hartig, W. Rasmussen, R. Schieder, and H. Walther, Z. Phys. A 278, 205 (1976).

B. Optical Nutation (ON) or Rabi Flopping

1. Observation of fluorescence after rotation of the polarization vector by a coherent pulse:

ON1. H. M. Gibbs, Phys. Rev. Lett. 29 459 (1972).

2. Time domain nutations following Stark switching:

ON2. R. G. Brewer and R. L. Shoemaker, Phys. Rev. Lett. 27, 631 (1971).

C. Adiabatic Rapid Passage (ARP)
Population inversion by optical ARP:

ARP1. M. M. T. Loy, Phys. Rev. Lett. 32, 814 (1974).

D. Free Induction Decay (FID)

FID1. R. G. Brewer and R. L. Shoemaker, Phys. Rev. A 6, 2001 (1972).

E. Photon Echoes (PE)

1. First experiment in ruby:

PE1. N. A. Kurnit, I. D. Abella, and S. R. Hartmann, Phys. Rev. Lett. 13, 567 (1964).

2. By Stark switching: see ON2 above.

B, D. and E are summarized in COT1. R. G. Brewer, Phys. Today 30, 50 (1977).*

II. THICK-SAMPLE EXPERIMENTS (theory must include effect of field on atoms and vice-versa).

A. Self-induced transparency (SIT)

1. Small-area linear propagation--absorption notch:

SIT1. J. M. Friedman, H. M. Gibbs, T. N. C. Venkatesan, B. Bölger, D. Polder, and M. F. H. Schuurmans, Opt. Commun. 20, 183 (1977).

2. Clean experiment in Rb showing pulse breakup and peak amplification:

SIT2. H. M. Gibbs and R. E. Slusher, Phys. Rev. Lett. 24, 638 (1970).*

B. Superfluorescence (SF)

1. First observation (in HF):

SF1. N. Skribanowitz, I. P. Herman, J. C. MacGillivray, and M. S. Feld, Phys. Rev. Lett. 30, 309 (1973).

2. Single-pulse SF in Cs:

SF2. H. M. Gibbs, Q. H. F. Vrehen, and H. M. J. Hikspoors, Phys. Rev. Lett. 39, 547 (1977).*

3. Direct measure of initial tipping angle:

SF3. Q. H. F. Vrehen and M. F. H. Schuurmans, Phys. Rev. Lett. 42, 224 (1979).

4. Quantum fluctuations in SF delay times:

SF4. Q. H. F. Vrehen and J. J. der Weduwe, Phys. Rev. A 24, 2857 (1981).

5. Simulation including transverse effects and quantum fluctuations agrees with Cs data:

SF5. E. A. Watson, H. M. Gibbs, F. P. Mattar, M. Cormier, Y. Claude, S. L. McCall, and M. S. Feld, Phys. Rev. A, to be published.

6. Single-mode SF in a cavity:

SF6. J. M. Raimond, P. Goy, M. Gross, C. Fabre, and S. Haroche, Phys. Rev. Lett. 49, 1924 (1982).

C. Optical Bistability (OB)

1. First observation (in Na):

OB1. H. M. Gibbs, S. L. McCall, and T. N. C. Venkatesan, Phys. Rev. Lett. 36, 1135 (1976).

2. Review:

OB2. H. M. Gibbs, S. L. McCall, and T. N. C. Venkatesan, Opt. News 5, 6 (1979).*

3. Room-temperature excitonic OB in a GaAs--AlGaAs superlattice etalon:

OB3. H. M. Gibbs, S. S. Tarng, J. L. Jewell, D. A. Weinberger, K. Tai, A. C. Gossard, S. L. McCall, A. Passner, and W. Wiegmann, Appl. Phys. Lett. 41, 221 (1982). *

4. Optical chaos:

OB4. H. M. Gibbs, F. A. Hopf, D. L. Kaplan, and R. L. Shoemaker, Phys. Rev. Lett. 46, 474 (1981).

OB5. H. M. Gibbs, F. A. Hopf, D. L. Kaplan, M. W. Derstine, and R. L. Shoemaker, SPIE 317, 297 (1981).

5. Optical computing:

OB6. E. Abraham, C. T. Seaton, and S. D. Smith, Sci. Am. 248(2):85 (1983).*

*Attached

physics today

COT1

Coherent optical transients

A new branch of optical spectroscopy that deals with the optical analogs of spin transients such as NMR is providing unique ways to explore dynamic interactions in optically excited atoms, molecules and solids.

Richard G. Brewer

The dynamics of nuclear spins in atomic and molecular environments have been examined in exquisite detail over the past 27 years by the methods of pulsed nuclear magnetic resonance.[1] The early discovery of the spin echo by Erwin Hahn[2] and the transient nutation effect by Henry Torrey[3] initiated the field by introducing coherent transient phenomena to radio-frequency spectroscopy. An entire class of coherent spin transients could be observed by a simple variation of the rf pulse sequence, and from the decay characteristics the various spin-dephasing mechanisms could be examined separately. In short, these methods allowed decomposition of the spin-transition linewidth into its broadening components, and also offered new and versatile ways for performing high-resolution rf spectroscopy.

Optical coherence is also a mature subject. Well known examples predating the laser are Young's two-slit interference effect, which demonstrates spatial coherence; the Michelson interferometer, which demonstrates temporal interference, and the Brown–Twiss experiment, which demonstrates an intensity-correlation effect. With laser light, however, a new class of optical coherence phenomena is now at hand, consisting of effects that are the *optical analogs* of spin transients. In this article I review this new branch of optical spectroscopy, which is providing unique ways for exploring dynamic interactions in optically excited atoms, molecules and solids.

The possibility of bringing the methods of pulsed NMR to the optical region was not immediately obvious. Because coherent radiation is required, optical studies were excluded prior to the laser, that is, before 1960. Furthermore, it was not clear whether optical electric-dipole transitions behaved in the same way as the rf magnetic-dipole transitions of spin systems. This situation was clarified in a well known paper[4] of Robert Dicke, who showed that the two are equivalent. In either case, a collection of two-level quantum systems can be prepared coherently in superposition states, and these constitute a phased array of dipoles (electric or magnetic), which can emit coherent radiation as prescribed by Maxwell's equations.

The photo on the cover of this issue of PHYSICS TODAY shows one example of a coherent transient in the optical region; it is observed by a laser frequency-switching technique described below.

Richard G. Brewer is an IBM Fellow at the IBM Research Laboratory in San Jose, California.

Maxwell–Bloch equations

The equivalence of magnetic- and electric-dipole transients was further demonstrated by Richard Feynman, Frank Vernon and Robert Hellwarth,[5] who transformed the Schrödinger equation into the three-dimensional vector equation

$$\frac{d\beta}{dt} = \omega \times \beta \qquad (1)$$

This has the form of the classical torque equation of motion for a spin precessing in a magnetic field and was used originally by Felix Bloch[6] to describe NMR. Equation 1 is commonly referred to as the Bloch equation. It is a geometric representation of a two-level quantum system interacting resonantly with a radiation field, acting either through an electric- or a magnetic-dipole interaction. The precessional motion of the Bloch vector β about an effective field ω (in frequency units) therefore applies to either situation, where we understand that the coordinate system in equation 1 rotates with the angular frequency of the radiation field about the z axis.

For the spin-½ case, the Bloch vector β is a magnetic dipole moment with three projections in real space, and the effective field ω is the vector sum of a static magnetic field (along the z axis) and an rf magnetic field (along the x axis) in the rotating frame, all multiplied by the gyromagnetic ratio.

For a two-level quantum system interacting with an optical wave, the Bloch vector

$$\beta = iu + jv + kw \qquad (2)$$

does not lie in physical space, but rather in a mathematical space with components

$$u = \tilde{\rho}_{12} + \tilde{\rho}_{21}$$
$$v = i(\tilde{\rho}_{21} - \tilde{\rho}_{12}) \qquad (3)$$
$$w = \rho_{22} - \rho_{11}$$

where ρ is the density matrix and the rapidly oscillating factor is removed with the substitution $\rho_{12} = \tilde{\rho}_{12}\exp[i(\Omega t - kz)]$. This assumes an electric-dipole interaction $V = -\mu \cdot E$ for an optical field $E = E_0 \cos(\Omega t - kz)$, which resonantly excites a transition $1 \rightarrow 2$ having a dipole matrix element μ_{12} and a transition frequency ω_{21}. Here, u and v represent the in-phase and out-of-phase components of the optically induced dipole

$$p = \mathrm{Tr}(\mu\rho) \qquad (4)$$

while the population difference of the transition levels is given by Nw, N being the atomic number density.

The effective field now takes the form

$$\omega = -i\chi + k\Delta \qquad (5)$$

where χ is the Rabi flopping frequency $\mu_{12}E_0/\hbar$. For the case of a moving atom with a velocity component v_z along the

Lasers in research

laser beam, the resonant tuning parameter, Δ, equals $\Omega + kv_z + \omega_{21}$ and the Doppler shift is kv_z.

The optically prepared dipoles given by equation 4 generate a coherent signal field

$$E_s(z,t) = \tilde{E}_s(z,t)e^{i(\Omega t - kz)} + \text{complex conjugate} \quad (6)$$

which obeys Maxwell's wave equation in the slowly-varying-envelope approximation

$$\frac{\partial E_s}{\partial z} = -2\pi i k N \langle \tilde{p} \rangle \quad (7)$$

when the sample is optically thin, the dipole amplitude being $\tilde{p} = \mu_{12}\tilde{\rho}_{12}$. Because atomic and molecular environments are always inhomogeneous, the dipoles radiate with a distribution of frequencies and exhibit temporal interference. The angular bracket in equation 7 therefore sums over the *inhomogeneous* line broadening, which is due to Doppler broadening for a gas and to crystalline strain broadening for a solid.

Decay phenomena

With the inclusion of damping [illegible] due to *homogeneous* line broadening the coupled Maxwell–Bloch equations are sufficiently general to describe [illegible] spin and optical coherent transient phenomena. Decay due to atomic [illegible] spontaneous [illegible] causes can [illegible] upper transition [illegible] respectively, [illegible] and [illegible] correspond to decay [illegible] and ρ_{22} [illegible] dipole and the off-diagonal [illegible] dephase at the rate

$$\gamma = \tfrac{1}{2}(\gamma_1 + \gamma_2) \quad (8)$$

There also exist processes that disrupt the phase of the dipole without depopulating either level so that equation 8 becomes

$$\gamma = \tfrac{1}{2}(\gamma_1 + \gamma_2) + \gamma_\phi \quad (9)$$

where γ_ϕ expresses the rate of phase interruptions.

When the radiative frequency changes with time because of spectral diffusion within the inhomogeneous line shape, the equations of motion must also be modified to allow for a decay that is no longer a simple exponential (see equation 11, below). In the language of NMR, the dipole terms u and v decay at the rate $1/T_2$ and the population term w decays at the rate $1/T_1$. In the above terms $\gamma = 1/T_2$, but T_1 is defined only when w is characterized by the single decay rate $1/T_1$, for example, when $\gamma_2 = \gamma_1$ or $\gamma_1 = 0$. The description in terms of T_1 and T_2 appears to be valid for transitions of molecular vibrational states in the infrared, as in NMR, but in the visible and ultraviolet regions the spontaneous emission rate can be large so that γ_1 and γ_2 are required,[8] as well as equations 8 and 9.

Echoes, free induction decay, nutation

The spin-echo concept, extended to the optical region in 1964 by Norman Kurnit, Isaac Abella and Sven Hartmann, was the first example of this class of optical coherence effects.[9] The group irradiated a ruby crystal with *two* short pulses of coherent light from a ruby laser and observed *three* equally spaced pulses in transmission, as shown in figure 1. The third pulse was a delayed spontaneous burst of coherent light, which they called a *photon echo* by analogy with the spin echo.

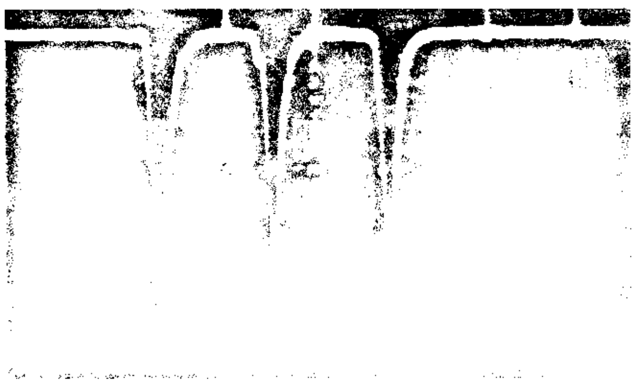

[illegible]

These studies revealed that the electron spin of the optically excited chromium ion of ruby dephased due to the presence of the surrounding aluminum nuclei through the mutual flipping of the electronic and nuclear spins. The photon-echo method has been applied also in other ways and to other systems, for example, by Hartmann and co-workers to photon-echo nuclear double resonance in ruby and most recently to low-temperature organic solids.[10]

An example of the photon-echo effect in a molecular gas[11] is shown in figure 2. The photon echo is an interference effect involving a coherent set of oscillating dipoles that dephase in the first pulse interval because of a spread in their frequencies (destructive interference) and rephase in the second pulse interval (constructive interference). The Bloch vector model shows this symmetric time behavior as a sequence of four precessional motions in figure 2 where the solutions of equation 1 are obtained by inspection.

Nutation For an initial laser pulse sufficiently long and intense, an atom will be driven first to the upper state (stimulated absorption) and then back to the lower state (stimulated emission), the cycle repeating thereafter until the end of the pulse. Since the laser beam is alternately absorbed and emitted by the sample, the intensity of the transmitted beam will display an oscillation as shown[11] in figure 3. This is the optical analog of the spin-nutation transient; it was first seen by G. B. Hocker and Chung Tang,[12] using a pulsed CO_2 laser, in an infrared transition of SF_6.

In terms of equation 1, the Bloch vector β points in the $-z$ direction for an atom initially in the lower state. With the application of a pulse, β precesses about the effective field $\omega = -i\chi + \mathbf{k}\Delta$, causing the level-population difference (the projection of β on the z axis) and the dipole (the projection of β on the x–y plane) to oscillate at $\omega = (\chi^2 + \Delta^2)^{1/2}$, the precession frequency. For atoms exactly on resonance ($\Delta = 0$), the precession frequency is the Rabi frequency χ, and the higher the light intensity the faster the oscillation.

If the pulse width t_1 is now reduced so that the precession angle χt_1 equals $\pi/2$, the Bloch vector of the resonant group will be totally in the x–y plane at the end of the pulse and the induced dipole will be a maximum, as in part **a** of figure 2. From equation 4, the off-diagonal element ρ_{12} will be a maximum also, corresponding to an equal admixture of the upper- and lower-state wave functions.

Free induction decay Immediately after the pulse, the dipoles are in phase and, according to equations 6 and 7, emit an intense coherent beam of light. This emission, shown in figure 4, was demonstrated initially by Richard Shoemaker and me[13]; it is the optical analog of the free induction decay first seen by Hahn in NMR. Notice that because the fields of the N dipoles add in phase, the emission intensity will vary as N^2 and so will far exceed spontaneous emission, which varies as N. Because of momentum (or $\mathbf{k}$) conservation, coherent emission can only occur in the forward direction.

In short, the emission due to free induction decay resembles the laser light that produced it, but with one difference: Because of inhomogeneous line broadening the dipoles radiate with a distribution of frequencies and thus interfere as time evolves, causing the emission to decay. The dephasing behavior of these frequency "packets" is seen in figure 2b, which shows the Bloch vector processing about $\omega = \mathbf{k}\Delta$ (since $\chi = 0$) for different frequencies Δ. We will now see that the echo is a free induction decay that has rephased.

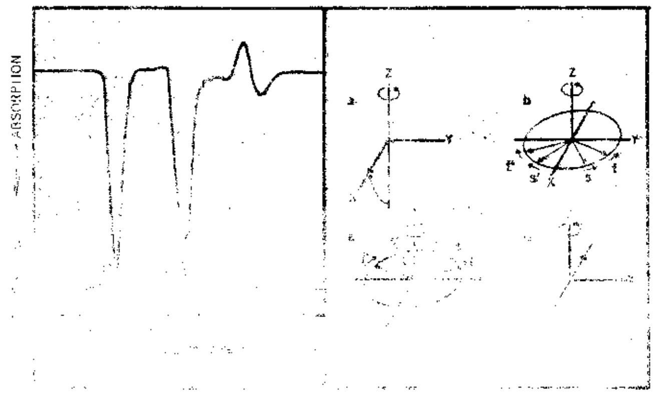

[illegible] Figure 2

Photon echo The second laser pulse tips the Bloch vector so that the sign of the dipole phase is reversed. This is shown in figure 2c for the resonance case, where the pulse duration t_2 gives a precession angle $\chi t_2 = \pi$. Other tipping angles and Δ's give echoes with smaller amplitudes. Following the second pulse, each Bloch vector in figure 2c precesses about the effective field $\omega = \mathbf{k}\Delta$ in the same sense as during the first pulse interval, but because the slow packets (labelled "s" in the figure) lead the fast ones, "f," it is clear that all packets will come into phase precisely at time 2τ, where τ is the pulse delay time. At this point the sample has a macroscopic dipole moment and will emit a burst of coherent light—the photon echo. By this dephasing–rephasing mechanism, the echo amplitude is unaffected by the large inhomogeneous linewidth, whereas the irreversible dephasing effects of homogeneous broadening remain.

Stark switched molecules

Optical studies have progressed rather slowly compared to the field of spin transients, because pulsed lasers are more difficult to control than rf pulse generators. A new method for observing coherent optical transients, particularly in the infrared, was introduced[11] by Shoemaker and me in 1971, and possesses several distinct advantages. In this case, the *exciting laser radiation is cw* and the *molecular level splitting is pulsed.* The apparatus is diagrammed in figure 5.

The underlying idea rests on the fact that molecules at a pressure of a few millitorr can exhibit exceedingly sharp optical resonances. Laser light, which is essentially monochromatic, will be strongly absorbed only when its frequency closely matches, to one part in 10^8–10^9, the molecular resonance frequency. If by some method the molecular transition frequency is shifted suddenly outside its homogeneous linewidth, the absorption can be switched on or off nonadiabatically. The switching mechanism used is the Stark effect, in which the application of a [illegible] field allows molecules [illegible] or away from the laser frequency. Instead of using pulsed [illegible] to control, the [illegible] energy-level spacing [illegible] [illegible]

[illegible] transients [illegible] figure [illegible] been [illegible] for [illegible] $C^{13}H_3F$ vibration–rotation [illegible] in the 10-micron infrared region [illegible] which will be referred to throughout [illegible] article. The beam from a stable cw

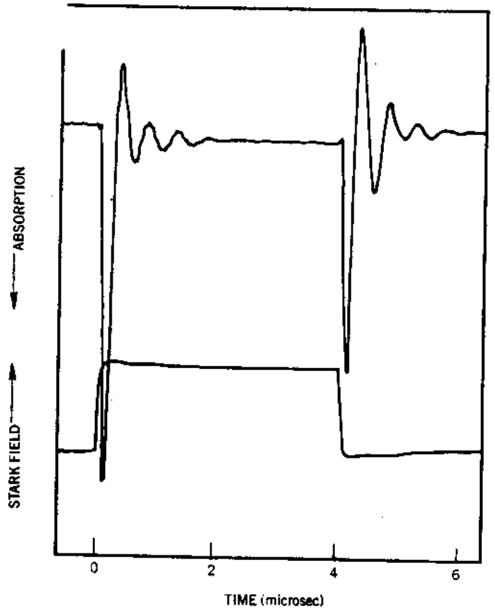

The optical nutation effect in methyl fluoride, $C^{13}H_3F$, irradiated by a carbon-dioxide laser at 9.7 microns. The apparatus for this experiment as well as that of figure 2 is shown schematically in figure 5. The Rabi oscillations appear here because the 35-volt/cm Stark pulse (colored line) is longer than those in figure 2. From R. G. Brewer and R. L. Shoemaker, reference 11. Figure 3

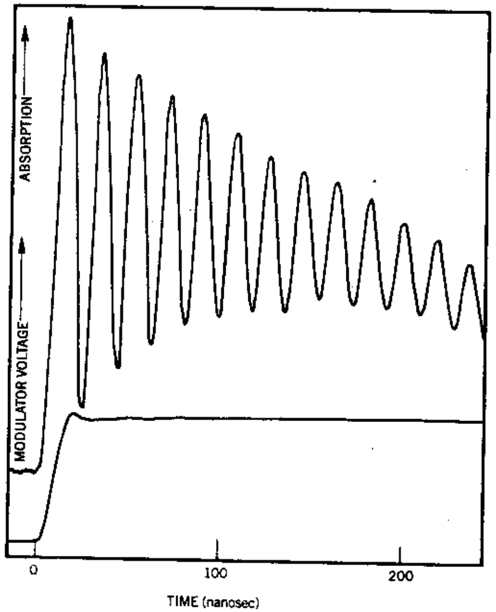

Optical free induction decay in I_2 vapor produces a heterodyne beat signal with frequency-shifted laser light. The sample is prepared with 5896-Å light from a cw dye laser; it radiates coherently when the frequency is abruptly switched 54 MHz by a 100-volt pulse. The slowly varying background is a nutation signal from a second velocity group. Figure 9 shows the experimental arrangement. (Ref. 18). Figure 4

CO_2 laser passes through the gas sample, which is contained in a Stark cell, before striking a photodetector that monitors the absorption or emission transients.

Imagine in figure 6 that, prior to a Stark pulse, a laser with frequency Ω selects from a molecule's Doppler line shape a particular velocity group v_z, which it coherently prepares under steady-state conditions. When a Stark pulse appears, this group is switched out of resonance and freely radiates an intense, coherent beam of light at frequency Ω' in the forward direction—the free-induction-decay transient. At the same time, a second velocity group v_z' will be switched into resonance and will alternately absorb and emit laser radiation—the nutation effect. If two Stark pulses are applied, the group v_z emits a third pulse—the photon echo.

The important advantages inherent in the Stark switching technique now become evident:

▶ The transient observed is the desired coherent transient itself, and the difficulty of separating a small transient signal from a time-coincident laser pulse of large amplitude is avoided.

▶ Heterodyne detection occurs because the emission transient is displaced in frequency from the laser light by the Stark shift and together with the laser beam strikes a photodetector. This increases the free-induction-decay and echo signals by about three orders of magnitude and facilitates measuring their decay.

▶ The entire class of coherent optical transient effects can be monitored, because the electronic pulse sequence and pulse shape can be tailored conveniently to the particular experiment of interest. To date, some ten different coherent optical transient effects have been observed in this way.[14]

Molecular collisions

The Stark switching method is well suited to the study of molecular collision phenomena.[15] Elastic and inelastic scattering can be examined easily with two-pulse echoes and without the complication of Doppler broadening. This work complements the more elaborate molecular-beam technique and contrasts with traditional steady-state linewidth measurements, in which the broadening mechanisms are rarely disentangled. The two-pulse sequence of figure 2 provides two independent measurements as the pulse delay time is advanced.

▶ The echo amplitude decreases be[illegible] collisions dephase the coherent [illegible] [illegible]

[illegible] dayed [illegible] grows, due to collisions that partially restore the equilibrium population from the imbalance created by the first pulse.

The delayed nutation and echo amplitudes for $C^{13}H_3F$ are shown in figure 7 as a function of pulse delay time. The nutation signal (upper curve) displays the decay time (T_1) for inelastic collisions, the cross section being about 500 Å^2. Elastic collisions, on the other hand, alter the molecular velocity, causing the echo signal to deviate from the upper curve. Because a collision-induced velocity change Δv_z translates as a Doppler shift $k\Delta v_z$ and a corresponding phase shift $k\Delta v_z t$ in time t, it is clear that even if Δv_z is small the dipoles will eventually get out of phase.

Writing the echo electric field in the form

$$E \propto \langle \exp(ik\Delta v_z t) \rangle$$

where ⟨ ⟩ denotes a collision average, we can use a simple Brownian-motion argument[15] to derive the echo time dependence due to elastic collisions. Let Δu be [illegible] times the rms change in velocity per collision and τ the pulse delay time. [illegible] $\tau \gg 1$, any collision produces destructive phase interference so that the [illegible] contribution to the field aver[illegible] [illegible] survives wil[illegible] the one wh[illegible] [illegible] [illegible] to the time [illegible] [illegible] [illegible] the [illegible] probability is $e^{-\Gamma t}$, where Γ is the rate of elastic collisions, one finds for long times

$$E(t = 2\tau) \propto \exp(-\Gamma t) \qquad \text{when} \quad k\Delta u\tau \gg 1 \qquad (10)$$

If, on the other hand, $k\Delta u\tau$ is much less than 1, each collision produces a small phase change such that $E \propto 1 - \frac{1}{2}k^2\langle(\Delta v)^2\rangle\tau^2$, where $\langle \Delta v \rangle = 0$. With the collision average $\langle(\Delta v)^2\rangle = \Gamma t \Delta u^2/2$, we get for short times

$$E(t = 2\tau) \propto \exp[-\Gamma t^3(k\Delta u)^2/16] \qquad \text{when} \quad k\Delta u\tau \ll 1 \qquad (11)$$

It agrees essentially with a more rigorous theory based on the Boltzman transport equation.[15]

These calculations also agree with the experiments of figure 7 and constitute primary evidence that elastic molecular collisions involving small changes in velocity *play a crucial role in infrared photon echoes.* The cubic decay law (equation 11) is reminiscent of the dephasing that occurs in spin echoes when spin diffusion in liquids takes place in a magnetic-field gradient.[2] In these optical experiments diffusion occurs in velocity space due to low-angle elastic scattering, for which the characteristic velocity jump per collision in $C^{13}H_3F$ is only Δu = 85 cm/sec and the corresponding total cross section is about 430 Å^2.

Carr–Purcell echoes A variation on this theme is to replace the two-pulse echo by an n-pulse echo sequence, which is easily done by applying $n + 1$ Stark pulses.[15] If the pulse interval τ is short enough, velocity or spectral diffusion can be made negligible and the decay time of the echo envelope [illegible] the residual [illegible] [illegible] [illegible] from the coincidence of the Carr–Purcell and nutation-decay curves, that $T_2 = T_1$. The n-pulse photon echo is an optical version of the NMR method of Herman Carr and Edward Purcell.[16]

The basic concept can be explained by noticing that for an n-pulse echo train with short pulse intervals τ, the amplitude of the last echo at time $t = 2n\tau$ is given by the nth power of the field E in equation 11; that is, $\{\exp(-8K\tau^3)\}^n = \exp(-Kt^3/n^2)$. In comparison to that given by equation 11 for a two-pulse echo over the same time interval t, it is evident that the Carr–Purcell decay time is n^2 times longer.

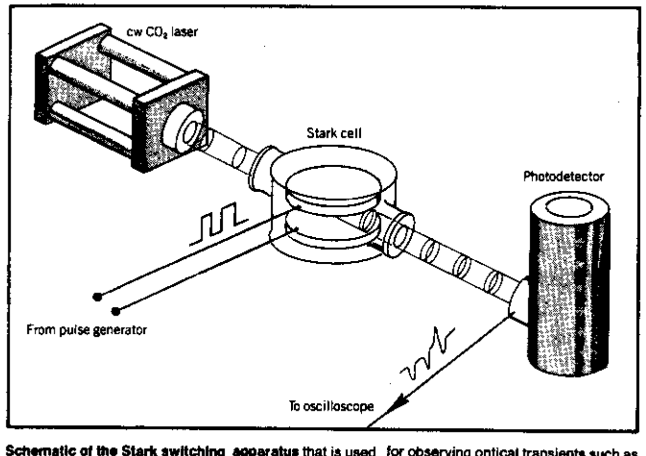

Schematic of the Stark switching apparatus that is used for observing optical transients such as those illustrated in figures 2 and 3. From reference 11. Figure 5

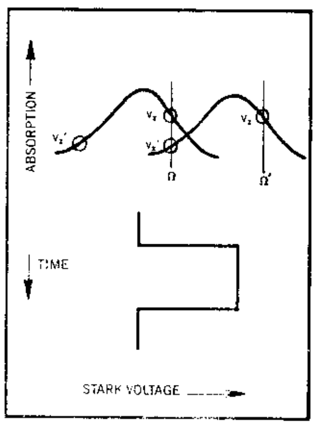

Stark switching principle for a Doppler-broadened transition. The [illegible], of fixed frequency Ω, initially [illegible]tes molecules of velocity v_z. A Stark pulse that [illegible] shifts the molecular transition frequency from the black to the colored curve [illegible] the velocity group v_z to emit the free induction decay [illegible] at frequency Ω' [illegible] the group [illegible] velocity v_z' exhibits nutation. [illegible] pulses, the [illegible] v_z' emits [illegible] echo. Figure 6

Fourier-transform spectroscopy

The method of Fourier transforming transient phenomena from the time to the frequency domain has proven to be an extremely versatile technique in pulsed nuclear magnetic resonance. With it, ultrahigh-resolution NMR spectroscopy can be performed quickly and with high sensitivity in a set of densely spaced lines. Furthermore, because the NMR signals display coherent transient behavior, dynamic information about nuclear spin interactions can be derived in a selective manner for each transition as well.

An application of this technique in the optical region[17] is shown in figure 8. The spectrum is obtained from several $C^{13}H_3F$ transitions that produce two-pulse photon echoes simultaneously. By advancing the pulse delay time, the echo decay for each transition can be monitored also. This yields a three-dimensional diagram of echo amplitude versus frequency and elapsed time. Measurements are performed with the Stark switching apparatus, which is now interfaced with a computer for rapid Fourier analysis. The four lines are actually heterodyne beat signals of the same Stark-split $C^{13}H_3F$ vibration–rotation transition, the ν_3 mode $(J,K,M) = (4,3,M) \to (5,3,M)$ mentioned earlier, each beat frequency being due to two transitions with $M \to M$ and $-M \to -M$. The lines are 170 kHz wide, are spaced at 0.83-MHz intervals and clearly display a Doppler-free behavior, as the Doppler width is 66 MHz. From echo and free-induction-decay measurements of this kind, elastic and inelastic scattering can be studied *independently* again, but since the lines are now resolved, the cross sections can be obtained as a function of *quantum state* and *molecular velocity.* This degree of flexibility offers stringent tests of existing scattering theories and is being used to study the force laws that dominate molecular collisions.

Laser frequency switching

Azriel Genack and I recently reported a general method for observing coherent transients in the visible–ultraviolet region[18] (Search and Discovery, PHYSICS TODAY, October 1976, page 17). The technique, diagrammed in figure 9, requires switching the laser frequency into or out of resonance with the sample; it is equivalent to the Stark switching method. However, when the source is a stable tunable cw dye laser, [illegible] approach is more universal in its application, particularly because the need for Stark tunable [illegible] is removed. Laser frequency [illegible] is exceedingly simple and can [illegible] merely by driving an elec-

tro-optic crystal (ammonium dihydrogen phosphate), which is inside the dye laser cavity, with the desired sequence of low-voltage pulses.

The time-dependent variations in the refractive index of the electro-optic element produce corresponding changes in the optical cavity length, and hence in the laser frequency. Dynamically the effect is equivalent to the Doppler shift the laser beam would experience on being reflected by a moving end mirror of the cavity. The frequency shift therefore occurs almost instantaneously. The switching time is limited by the transit time of light through the ADP crystal, about 50 picosec, and not by the rise time of the voltage pulse or by the laser-cavity ringing time, about 25 nanosec. In addition, the frequency-shifted light is stored in the optical cavity and amplified in the same way that the unshifted light was.

Clearly, a resonant sample exposed to frequency-switched laser light will experience coherent transient behavior. Because the experiment is controlled electronically, all of the advantages inherent in the Stark switching technique are preserved here as well. Moreover, with the large tuning range of the dye laser, measurements are equally feasible in atoms, molecules and solids.

In initial studies in molecular iodine vapor, effects such as free-induction-decay (figure 4), nutation and echoes are easily monitored in the visible. Because the signal-to-noise ratio is high, about 10^3, it has been possible to test the theory of these transient phenomena quantitatively and in complete detail. From two-pulse nutation and echo studies of I_2 it is found that elastic collisions are not of the velocity-changing type, as in the infrared, but rather are due to collision-induced frequency shifts. In this case, the echo decays exponentially with a decay rate given by equation 9, in contrast to equation 11. Apparently, excited electronic states are more sensitive to perturber-induced frequency shifts than vibrationally excited states are. This appears to be the first optical-coherence measurement of phase-interrupting collisions.

In a solid, laser frequency switching has been used at IBM to measure the dephasing time of coherently prepared impurity ions of praseodymium in a low-temperature LaF_3 host crystal.[19] Free-induction decay is monitored and possesses certain advantages over the echo technique. As can be seen in figure 4, the entire decay is obtained in a single burst following a step-function switching pulse. Because of the sensitivity offered by heterodyne detection, weak transitions can be studied at laser powers as low as 50 microwatts. At laser power levels, where $\chi^2 \ll 1/(T_1T_2)$, the free-induction-decay time is simply $\frac{1}{2}T_2$ where the $\frac{1}{2}$ factor arises because T_2 determines the inhomogeneous bandwidth during steady-state preparation and adds an additional $1/T_2$

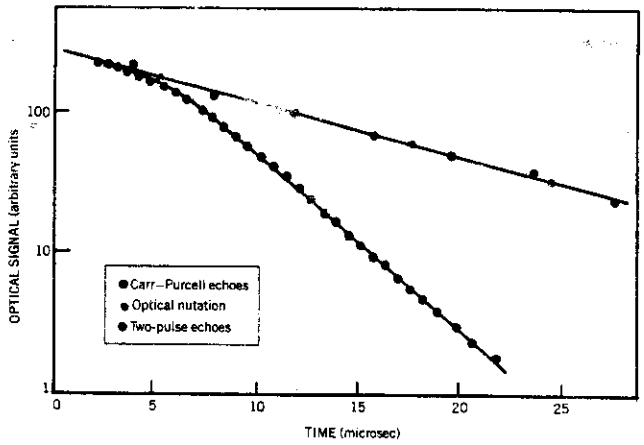

Decay curves for three coherent infrared transient effects, observed in $C^{13}H_3F$ by Stark switching. The Carr–Purcell and nutation curves coincide. From reference 15. Figure 7

decay rate. The rather long Pr^{3+} dephasing time of 0.38 microsec corresponds to an extremely narrow linewidth of 830 kHz (resolution: 6×10^8) and is unaffected by phonons below 4 K, power broadening, Pr^{3+}–Pr^{3+} interactions or the large inhomogeneous width of 4 GHz arising from crystal strains. On the other hand, it far exceeds the 640-Hz limit due to spontaneous radiative decay of the upper level.

Magnetic hyperfine interactions constitute a possible dephasing mechanism currently under study by several groups including Hartmann (Columbia University), Lynden Erickson (NRC, Ottawa) and Raymond Orbach (UCLA). Thus these measurements begin to invade a time scale ranging from microseconds to milliseconds and will impose significant demands on laser frequency stability.

At the other extreme, the fastest dephasing time measured by laser frequency switching is about 8 nanosec, as seen in the free induction decay of the sodium D lines. It will be challenging to see whether this method can be extended in the future to even shorter times, perhaps to the 50-picosec range.

Picosecond pulse generation

A related development, intense optical pulses of 30 picosec duration generated by free induction decay in a high-density gas, has attracted interest in laser fusion.[20] In the preparative step, a CO_2 laser pulse 200 nanosec long and 1 MW in power passes through a pair of lenses before resonantly exciting a CO_2 gas sample at a pressure of about 250 Torr. At a certain time during the pulse the excitation ends abruptly, due to dielectric breakdown of the gas in the focal region between the lenses; at this point free induction decay commences. Because nearly all of the laser light was absorbed during preparation, the emission will be intense initially and thereafter will decay in the time $T_2/(\alpha L)$ when $\alpha L > 1$; here α is the absorption coefficient and L the sample length. Hence, in this high-density regime, the decay can be considerably faster than the dipole-dephasing time T_2.

Two-photon transients

The one-photon processes considered up to this point are for the most part optical analogs of NMR transient phenomena. Coherent two-photon transients have been observed in the optical region also and provide additional information about dephasing processes.

Picosecond studies Foremost among the two-photon processes are the Raman transients, which were exploited in simple liquids by Wolfgang Kaiser and his coworkers,[21] who used picosecond laser pulses, as from a mode-locked neodymium glass laser of wavelength 1.06 microns. (See also the accompanying article by Marc Levenson on steady-state aspects of Raman scattering in this issue of PHYSICS TODAY.) Vibrational decay times on a picosecond time scale have been obtained by first generating a coherent vibrational excitation and Stokes light through the stimulated Raman process. A weak delayed second pulse then probes the remaining vibrational excitation by generating phase-matched anti-Stokes radiation. The vibrational dephasing time is monitored through the dependence of the anti-Stokes intensity on pulse delay time. In liquid carbon tetrachloride, for example, the totally symmetric vibrational mode shows a dephasing time T_2 of 3.6 picosec. Moreover, the decay exhibits beats at a frequency of about 10^{11} Hz, due to the different isotopic species Cl^{35} and Cl^{37}.

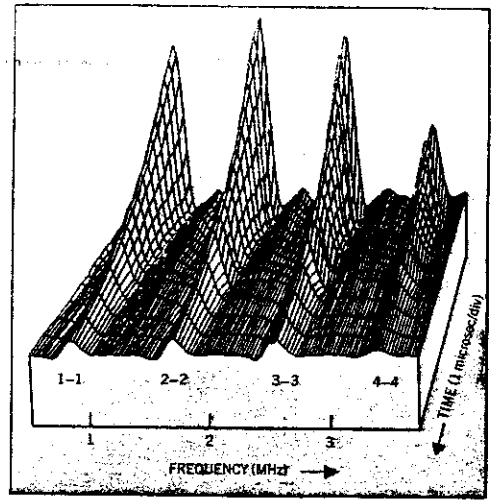

A Fourier-transform spectrum of $C^{13}H_3F$, derived from Stark-switched two-pulse photon echoes, shows beats in this three-dimensional diagram of echo amplitude as a function of frequency and pulse-delay time. The vibration–rotation transitions 1–1, 2–2, . . . , exhibit decay with increasing pulse delay time. From reference 17. Figure 8

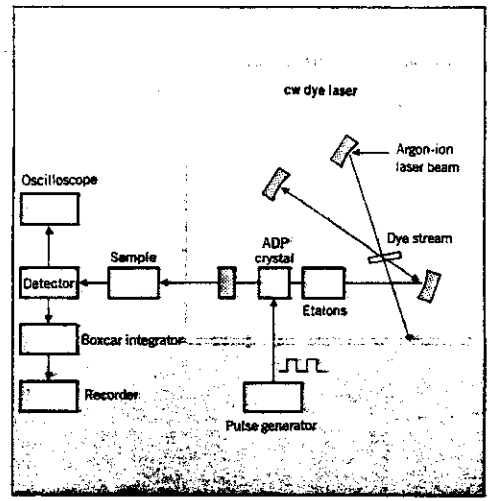

Laser frequency switching apparatus for observing coherent optical transients. In the box is a commercial cw dye laser with an electro-optical crystal of ammonium dihydrogen phosphate. When the crystal is driven by low-voltage dc pulses its refractive index changes, abruptly changing the laser frequency. From reference 18. Figure 9

Raman echoes Stimulated spin-flip Raman scattering has been used to induce coherent spin states[22] of bound donors in n-type CdS at 1.6 K, in the same way that vibrational modes are prepared coherently in molecular liquids. This is accomplished by exciting the sample with a pulsed dye laser at 4905 Å with two modes having a frequency difference $\omega_L - \omega_R = 32$ GHz, which is just resonant with a pair of Zeeman-split spin states. After pulse preparation the spins dephase, as in free induction decay, and if a second optical pulse is applied the spins will rephase, as in an echo experiment. The spin dephasing–rephasing behavior can be monitored optically by suitably delaying a weak probe laser pulse at 4880 Å to produce Stokes scattering. The probe Raman scattering is enhanced at the time the spins have rephased and is called the Raman echo. Echoes of this type, which were predicted by Hartmann, have been observed[22] with delay times to 162 nanosec in dilute samples of CdS (of density 8×10^{15} cm^{-3}).

Coherent Raman beats A different manifestation[23] of a two-photon transient can be found in a molecular gas with the Stark switching technique when three molecular levels are prepared initially in superposition by means of continuous laser radiation. We imagine that two of the levels (1 and 2) are degenerate and connect optically with a third (3) during a resonant steady-state preparative phase. With the sudden application of a dc Stark field, the molecular level degeneracy is broken and the laser beam is no longer in resonance with the one-photon transitions, $1 \leftrightarrow 3$ and $2 \leftrightarrow 3$. However, the laser beam can now scatter off the coherently prepared sample in a two-photon process $1 \leftrightarrow 2$; that is, coherent forward Raman scattering can occur in the presence of the same laser field during the nonresonant condition. The two beams—the laser beam with frequency Ω and the Raman light with frequency $\Omega \pm \omega_{21}$—strike a photodetector, where they produce a coherent beat at frequency ω_{21}. This is just the level splitting between initial and final states in the two-photon process.

From energy conservation, we see that the first-order Doppler shift kv_z in the first half of the two-photon process ($1 \leftrightarrow 3$) essentially cancels that of the second half ($3 \leftrightarrow 2$), making the overall process $1 \leftrightarrow 2$ independent of Doppler shift. As a result, inhomogeneous dephasing and elastic collisions that change the molecular velocity do not alter the decay rate of the Raman beat signal. That the decay will be determined only by inelastic collisions, in contrast to the two-pulse echo results, is corroborated by theoretical arguments and experiments.[15,23]

Two-photon nutation A two-photon transient can be induced also by the sudden application of two light pulses of frequency Ω_1 and Ω_2, such that the transition $1 \rightarrow 2$ satisfies the resonance condition $\Omega_1 + \Omega_2 = \omega_{21}$. In this case the energy of the intermediate level 3 lies roughly half way between 1 and 2, and the two waves must be counterpropagating so that the Doppler shifts nearly cancel, as in the Raman beat effect. Exact pulse or steady-state density-matrix solutions[23] for the three-level problem show in fact that the Raman beat effect with a single beam and two-photon absorption of oppositely directed laser beams are basically the same phenomenon, the difference being one of level configuration. The pulse solutions also reduce in an appropriate limit to a simple Bloch vector model,[24] resembling equation 1, as it involves only the initial and final states in the overall transition $1 \rightarrow 2$. The intermediate level does not enter explicitly when the pulses are applied slowly (adiabatically) with respect to the frequency offset of the intermediate level, that is, when the intermediate transitions are nonresonant.

Michael Loy[25] has observed an infrared two-photon vibrational transient of this type in ammonia, which is induced by two counterpropagating CO_2 laser pulses. The transient oscillates because of the nutation effect, in quantitative agreement with the two-photon vector model. It is interesting that two-quantum transients in NMR are now also being explored.

Milliseconds to picoseconds

New ways for observing a class of coherent optical transient phenomena—measurements that resemble pulsed NMR transients—are now possible with the availability of laser radiation. Other novel effects[26] such as superradiance, quantum beats, adiabatic rapid passage and self-induced transparency, which were not discussed here, could have been included as well. Many of these coherence effects are just beginning to be useful in examining energy transfer and de-

phasing processes in optically excited atoms, molecules and solids, with time scales spanning the range from milliseconds to picoseconds.

* * *

The author gratefully acknowledges the thoughtful comments and criticisms of A. Z. Genack and A. Szöke. This work was supported in part by the US Office of Naval Research.

References

1. A. Abragam, *The Principles of Nuclear Magnetism*, Oxford, London (1961).
2. E. L. Hahn, Phys. Rev. **80**, 580 (1950); PHYSICS TODAY, Nov. 1953, page 4.
3. H. C. Torrey, Phys. Rev. **76**, 1059 (1949).
4. R. H. Dicke, Phys. Rev. **93**, 99 (1954).
5. R. P. Feynman, F. L. Vernon, R. W. Hellwarth, J. Appl. Phys. **28**, 49 (1957).
6. F. Bloch, Phys. Rev. **70**, 460 (1946).
7. M. Sargent III, M. O. Scully, W. E. Lamb Jr, *Laser Physics*, Addison-Wesley, Reading, Mass. (1974), page 84.
8. A. Schenzle, R. G. Brewer, Phys. Rev. A **14**, 1756 (1976).
9. N. A. Kurnit, I. D. Abella, S. R. Hartmann, Phys. Rev. Lett. **13**, 567 (1964); Phys. Rev. **141**, 391 (1966); S. R. Hartmann, Scientific American, April 1968, page 32.
10. T. J. Aartsma, D. A. Wiersma, Phys. Rev. Lett. **36**, 1360 (1976); A. H. Zewail, T. E. Orlowski, D. R. Dawson, Chem. Phys. Lett. **44**, 379 (1976).
11. R. G. Brewer, R. L. Shoemaker, Phys. Rev. Lett. **27**, 631 (1971).
12. G. B. Hocker, C. L. Tang, Phys. Rev. Lett. **21**, 591 (1968).
13. R. G. Brewer, R. L. Shoemaker, Phys. Rev. A **6**, 2001 (1972).
14. R. G. Brewer, in *Proceedings of the Les Houches Summer School Lectures, Volume I, Applications of Lasers to Atomic and Molecular Physics*, Les Houches, France, 1975 (R. Balian, S. Haroche, S. Liberman, eds.), North-Holland (in press).
15. P. R. Berman, J. M. Levy, R. G. Brewer, Phys. Rev. A **11**, 1668 (1975).
16. H. Y. Carr, E. M. Purcell, Phys. Rev. **94**, 630 (1954).
17. S. B. Grossman, A. Schenzle, R. G. Brewer, Phys. Rev. Lett. **38**, 275, 1977.
18. R. G. Brewer, A. Z. Genack, Phys. Rev. Lett. **36**, 959 (1976).
19. A. Z. Genack, R. M. Macfarlane, R. G. Brewer, Phys. Rev. Lett. **37**, 1078 (1976).
20. E. Yablonovitch, J. Goldhar, Appl. Phys. Lett. **25**, 580 (1974); **30**, 158 (1977).
21. A. Laubereau, G. Wochner, W. Kaiser, Phys. Rev. A **13**, 2212 (1976).
22. P. Hu, S. Geschwind, T. M. Jedju, Phys. Rev. Lett. **37**, 1357 (1976).
23. R. L. Shoemaker, R. G. Brewer, Phys. Rev. Lett. **28**, 1430 (1972); R. G. Brewer, E. L. Hahn, Phys. Rev. A **11**, 1641 (1975).
24. D. Grischkowsky, M. M. T. Loy, P. F. Liao, Phys. Rev. A **12**, 2514 (1975).
25. M. M. T. Loy, Phys. Rev. Lett. **36**, 1454 (1976).
26. L. Allen, J. H. Eberly, *Optical Resonance and Two Level Atoms*, Wiley, New York (1975). □

OPTICAL BISTABILITY

OB2

INTRODUCTION

Recent transmission of 1.32-μm, 5-psec pulses through 1 km of optical fiber without significant dispersional distortion[1] has clearly demonstrated the high-bandwidth capability of using short optical pulses and optical fibers. In addition, propagating optical signals are not easily influenced by external electromagnetic fields. Both facts point to optical communication as an attractive information-transmission medium for the future. Commercial optical communication systems operating at 44.7 Mbit/sec now function quite satisfactorily, and studies of higher-rate systems are under way.[2] In all these systems, only the transmission is optical: regeneration, modulation, amplification, etc. are all accomplished electrically. Even in the present technology of integrated optics, in which light is generated, manipulated, and detected in thin-film waveguide structures on the same substrate,[3] most of the control is accomplished electrically. Other things being equal, all-optical control would permit simpler, efficient, and higher-speed information processing because the conversion of information from electricity to light and vice versa would be avoided. Optically bistable devices exhibit an intensity-dependent optical transmission and are able to perform optically controlled memory and switching operations and hence may be crucial to the success of all-optical systems. Discrete devices may be used singly or in combinations to form elements such as optically controlled modulators, oscillators, and logic gates.

Although the notion of all-optical communication and computation motivates much of the work, optical bistability is an interesting physical phenomenon in its own right. The search for optical nonlinearities needed for realizing optical bistability has led to interesting studies of the physics of several different nonlinear optical processes; in fact, the first few attempts to observe optical bistability failed because the nonlinear materials selected had inappropriate properties. An optically bistable system is analogous to a first-order phase transition under conditions far from thermal equilibrium. Finally, the fluorescence spectrum of atoms within an optically bistable cavity exhibits interesting features far different from those of isolated atoms.

In this article, optical bistability is defined and various classifications explained, a simple mathematical model of intrinsic dispersive bistability is presented, experimental examples of wireless all optical operations are given, hybrid devices are described, and possible future directions are summarized.

H. M. Gibbs and S. L. McCall are with Bell Laboratories, Murray Hill, New Jersey 07974. T. N. C. Venkatesan is with Bell Laboratories, Holmdel, New Jersey 07733.

WHAT IS OPTICAL BISTABILITY?

Any optical system that possesses two different steady-state transmission states for the same input intensity can be said to be optically bistable. This broad definition encompasses everything from burglar alarms to the most recent all-optical micrometer-sized GaAs device. However, in this article optical bistability will be examined only in transmission devices containing no inverted medium. In order for bistability to occur, the transmission must somehow depend on the *output* intensity, i.e., feedback is essential. If this feedback is purely optical, for example, if the nonlinear material is inside a Fabry-Perot cavity, the device and its bistability are described as *intrinsic*. If an electrical signal from a detector sensing the output is fed back to change the transmission, the device is described as *hybrid*. Optically bistable devices are also classified as *absorptive* or *dispersive*, depending on the nature of the predominant nonlinearity giving rise to the bistability.

All the early theoretical work and experimental attempts involved in-

OPTICS NEWS 5, 6 (1979).

H. M. Gibbs, S. L. McCall, and T. N. C. Venkatesan

trinsic and absorptive nonlinear media inside a Fabry–Perot resonator. A simplistic view of intrinsic absorptive optical bistability is as follows. At low input intensity, the intracavity absorber spoils the Q of the cavity, so the transmission is low and the light is mostly reflected by the input mirror. At sufficiently high input intensity I_I, the intensity TI_I reaching the absorber becomes large enough to begin to bleach it (T is the transmission of the mirror coating). As the absorber's transmission increases, light begins to reach the output mirror and to reflect back to help saturate the absorber. At the same time, constructive interference occurs, increasing the intensity inside the cavity. The absorber is bleached in a runaway manner. Further increases in the input are transmitted to the output. The device is now a high-Q cavity with an intense internal field. As the input intensity is reduced, this intracavity field is able to keep the absorber bleached down to lower input intensities than were required to turn on the device; a hysteresis cycle results.

Seidel proposed such a device as an extension of his work on similar effects in the microwave region.[4] Szöke [illegible] absorptive optical [illegible] demonstrated nonlinear [illegible], using SF_6 as [illegible] a CO_2 laser, but did not see bistability.[5] They proposed several applications and derived the bistability condition $\alpha L/T > 8$, where αL is the low-intensity value of the homogeneously broadened saturable absorption and T is the mirror transmission. Austin and DeShazer[6] and Spiller[7] studied transmission of nonlinear Fabry–Perots containing absorbing dyes; the failure to see bistability was attributed to unsaturable background absorption, which analysis showed could greatly modify the conditions for bistability. McCall[8] further analyzed absorptive bistability by studying the effects of inhomogeneous broadening, standing waves, and transverse modes. His work stimulated the first observation of optical bistability, which began the rapid expansion of this exciting field.

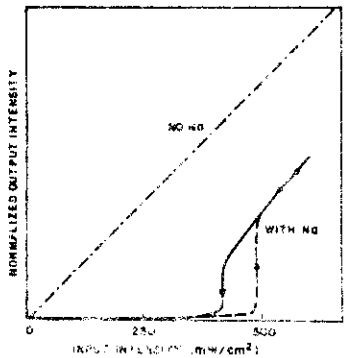

Fig. 1. Dispersive optical bistability in sodium vapor (Ref. 9).

FIRST OBSERVATION

The first observation of transmission optical bistability was made in 1974 in sodium vapor[9]; however, the principal mechanism was dispersive, not absorptive. In purely dispersive bistability, no intracavity absorption is present; the transmission at low intensities is made small by detuning the cavity resonance from the laser frequency. The device turns on when the intracavity intensity-dependent index of refraction shifts the cavity back to the laser frequency. As in absorptive bistability, a hysteresis results as the intracavity field of the "turned-on" device resists the turn-off as the input is reduced (see Fig. 1). Intrinsic absorptive optical bistability was barely seen at the highest intensity and only at particular frequencies where dispersive effects vanished. On the other hand, dispersive bistability was seen easily. Since all the intrinsic bistable devices reported so far work primarily dispersively, it is appropriate to present the following simple model of dispersive bistability.

SIMPLE MODEL OF INTRINSIC DISPERSIVE OPTICAL BISTABILITY

From Fig. 2, one can readily verify the following boundary conditions[8] for a lossless Fabry–Perot cavity:

$$E_T = \sqrt{T}E_F(L), \tag{1}$$

$$E_B L = \sqrt{R}E_F(L), \tag{2}$$

$$E_F(L) = \sqrt{T}E_I e^{i\phi/2} - \sqrt{R}E_B(L)e^{+i\phi}, \tag{3}$$

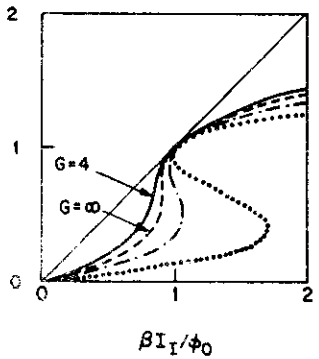

Fig. 3. Characteristic transfer function calculated from the simple dispersive model of Eqs. (4) and (5) for $R = 0.9$ ($N \approx 30$). The values of ϕ_0 are 0.158, 0.183, 0.224, and 0.316, respectively, from left to right. The $G = \infty$ curve separates the ac gain and bistable regions (Ref. 10).

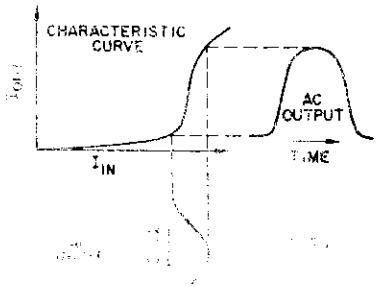

[illegible] ac gain in sodium vapor, [illegible] kHz [illegible] were observed. [illegible]

where ϕ is the round-trip phase and the plate reflectivity is $R = 1 - T$. Assume T to be small compared to unity. Combining these three equations and expanding in powers of ϕ, if $\phi^2 << 12$, one has approximately

$$I_I = (1 + R\phi^2/T^2)I_T, \tag{4}$$

relating the input intensity I_I and the output intensity I_T.[10] In general, the phase ϕ is a function of the intracavity intensity, which is proportional to the transmitted intensity I_T. A simplifying assumption is a linear dependence on I_T, so that

$$\phi = \beta I_T - \phi_0, \tag{5}$$

where β is a constant and ϕ_0 is an externally adjustable tuning parameter. This is the case for a nonlinear refractive index that arises from an optical Kerr effect or for a system that responds according to Bloch equations in the off-resonance limit. If

$$\phi_0 > \frac{\sqrt{3}T}{\sqrt{R}} \tag{6}$$

(for β positive), then there is a negative slope region, i.e., $dI_I/dI_T < 0$, around $I_T = 2\phi_0/3\beta$. The steady-state curve I_T versus I_I is s-shaped. For some values of I_I there are three steady-state values of I_T. Of these, only the two extreme values can be stable,[11] i.e., the system is bistable. The condition (6) may be written as $\phi_0 > \sqrt{3}\pi/N$, where N is the cavity finesse. One might have guessed that ϕ_0 of about one instrument width, $2\pi/N$, would be required so that the low-intensity transmission would be low. The minimum intensity-dependent phase shift is $\beta I_T = 2\phi_0/3$; the required intensity depends on the cavity finesse and the strength of the nonlinearity (β). Smaller values of ϕ_0 yield I_T versus I_I curves that exhibit regions of differential gain, where

$$\frac{dI_T}{dI_I} > 1. \tag{7}$$

Figure 3 shows plots of the Fabry–Perot [illegible] for various [illegible], showing the [illegible] from gain to [illegible] bistability [illegible] increasing the [illegible]

Fig. 5 Optical discriminator in room-temperature ruby (Ref. 13).

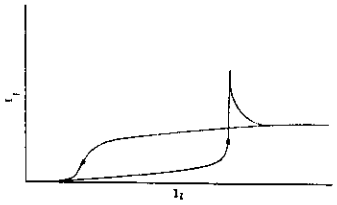

Fig. 6. Optical bistability and limiter action in a 2-mm-long etalon consisting of a polished Corning 3-142 filter with $R \approx 0.8$. In the on state, the output changes very little for a factor-of-4 change in the input. Note the spike in the transmission as the device turns on and the etalon's frequency of peak transmission is swept through the laser frequency. Similar results obtained in a 60-μm etalon of Corning 4-74 with $R = 0.9$ (Ref. 14).

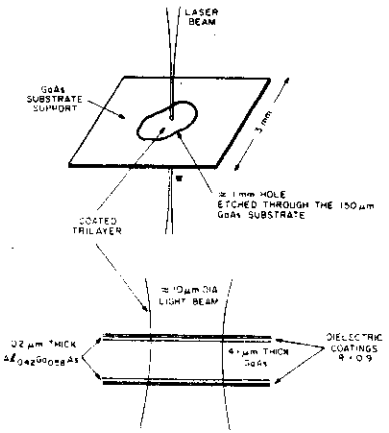

Fig. 7. GaAs–GaAlAs trilayer sandwich grown by molecular-beam epitaxy and used for optical bistability and optical modulation.

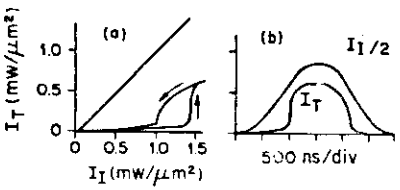

Fig. 8. (a) Optical memory in GaAs. (b) Time display of bistability in (a); the switch-on and switch-off times are both about 40 nsec (Ref. 15).

Fig. 9. Switch-on of GaAs optical bistability by 590-nm, sub-nsec pulse. The experimental parameters were adjusted so that switching did not occur in (a) but did in (b). The switch-on in (b) is expanded in (c), revealing a 1-nsec, detector-limited switch-on time. The spike in (a) and (b) is absent if the red probe beam is absent (Ref. 15).

in detail the transmission of a lossless Fabry–Perot containing a Kerr-effect nonlinearity. They predicted multiple-valued transmission-intensity characteristics and, in spherical-mirror cavities, reduced powers for bistability from self-induced waveguiding effects.

EXPERIMENTAL ALL-OPTICAL OPERATIONS

Intrinsic dispersive devices have been constructed using a variety of optical nonlinearities. In addition to bistability, other effects were observed in these systems. Differential gain action using hyperfine optical pumping in sodium vapor [9] in an 11-cm Fabry-Perot, thereby amplifying a weak signal beam, was observed (Fig. 4). Optical discrimination is shown in Fig. 5 that uses index changes caused by far-away but very strong ultraviolet bands when the R lines in ruby[13] are excited. By using optical discrimination, above-threshold signal pulses can be separated in a quantized way from below-threshold noise pulses. Optical limiting (Fig. 6) was demonstrated that utilizes thermally induced index changes arising from optical absorption in color filters[14] polished and coated to form Fabry–Perot etalons ranging from 2 mm to 60 μm in length. Thus a noisy input, with an intensity above the turn-on intensity, is stabilized. Most impressive is the optical memory or optical bistability observed in a 4.2-μm layer of GaAs (Ref. 15) between 0.2-μm $Al_{0.42}Ga_{0.58}As$ windows utilizing intensity-dependent contributions to the index of refraction from the free-exciton resonance in GaAs (Figs. 7 and 8); information can be stored and read optically. With a holding intensity of one mW/μm^2, the tiny ($\approx$ 15-μm-diameter laser-spot-diameter) optical memory element was switched from the off state to the on state in a detector-limited time of 1 nsec by a 589-nm, 200-psec pulse of 0.1 pJ/μm^2 (Fig. 9). The saturation of the free-exciton absorption is less than a picosecond by a picosecond pulse suggests switch-on times approaching a picosecond.[16] Switch-off times of 40 nsec were observed when the input was slowly decreased. Rapid switch-off by an optical pulse would be preferable if a mechanism could be found to permit it. Finally, the same semiconductor heterostructure (Fig. 7) and an above-bandgap control beam were used to gate a near-exciton-wavelength beam [17] (Fig. 10).

The GaAs–GaAlAs trilayers (Fig. 7) were grown by A. Gossard and W. Wiegmann by molecular-beam epitaxy, a method of building crystals one layer of atoms at a time. The layers are sufficiently parallel to form 15-μm-diameter optical cavities of finesse of about 15 with $R = 0.9$ coatings. The trilayers are illuminated perpendicularly, so that more than a thousand devices might be utilized in a 1-mm-diameter sample area with an appropriate heat sink. Interconnections might be simplified if planar devices and waveguides[3] could be constructed. Already Okuda *et al.* have analyzed saturable optical resonators with distributed Bragg reflectors.[18]

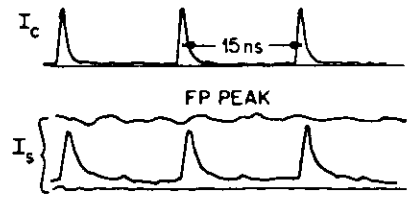

Fig. 10. Control of a 10-mW cw dye laser beam I_s by 2.5-W 514.5-nm 200-psec mode-locked Ar pulses I_c. Turn-on of the signal follows the integrated control pulse that sweeps the Fabry–Perot peak onto the signal wavelength (λ_s = 821.3 nm). The 2-nsec recovery time is related to the carrier lifetime. (10 K; $\lambda_{exciton} \simeq$ 818 nm) (Ref. 17).

HYBRID BISTABLE DEVICES

Kastal'skii[19] is apparently the first to propose the construction of an optically bistable device in which an intracavity electro-optic crystal introduces intracavity index changes proportional to the output intensity. Clearly a phase shift satisfying Eq. (5) results, so our simple model is applicable and all the operations previously discussed are possible. Smith and Turner[20] demonstrated dispersive hybrid optical bistability and differential gain, using feedback to an electro-optic crystal (see Figs. 11 and 12). Hybrid devices have been used to observe[21,22] the multiple-valued transmission predicted by Felber and Marburger. Garmire *et al.*[23] emphasize that optical feedback is unnecessary in a hybrid device since any optical element with a nonlinear transmission as a function of applied voltage can be made bistable if it is driven by a signal proportional to the output intensity. Mirrorless bistability has been demonstrated, using various electro-optic devices between two polarizers[22-24] and using a waveguide-directional coupler switch.[25] Integrated hybrid devices[25-27] have been constructed, but generally they are many millimeters in length and involve external power supplies, amplifiers, lenses, or diode arrays and hence are not yet truly integrated.

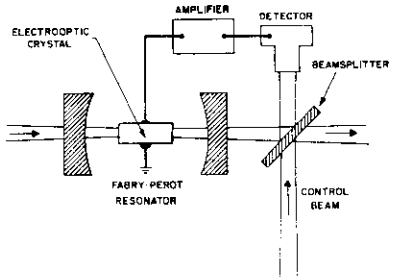

Fig. 11. Smith–Turner hybrid device with additional control beam (Ref. 21).

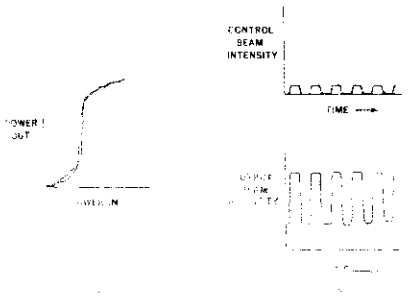

COMPARISON OF INTRINSIC AND HYBRID DEVICES

Hybrid devices may find specific applications when all-optical operation is not necessary. Since the feedback can be made strong by electrical amplification, the optical sensitivity of the device is limited by the statistics of the detector and the feedback loop. A self-contained hybrid device, i.e., one requiring no external power source, has been constructed, using an electro-optic waveguide structure with end mirrors to form a cavity with a finesse of 4. In the bistable mode of operation, obtained by an electrical feedback from a 21-element photovoltaic detector sampling part of the transmitted light, the switching time and [illegible] were 4 nsec and [illegible].[26] Use of

an avalanche detector and external power supply permitted 50-nsec switching with 0.5 pJ.[26] Mirrorless, hybrid optical bistable devices have also been reported,[22-24] simplifying integration and broadening the wavelength range. Since the hybrid devices do not utilize any material resonance, room-temperature operation is possible, and the wavelength of the incoming light need only be within the response curve of the photodetector used in the feedback loop. Whereas the mirrorless devices could use multimode or even incoherent light, the mirrored, hybrid devices are predominantly single mode because of the waveguide structure. Unfortunately, these hybrid devices are usually about a centimeter long in order to permit the required phase shifts to be obtained with reasonable voltages. This length imposes fundamental limitations on the speeds of these devices, which are further limited by the electronic feedback loops. Whereas the increased length requires fractions-of-an-angstrom input-wavelength stability for cavity-type devices, the mirrorless devices are not sensitive to small wavelength changes. But, because of the absence of the enhancing effects of a cavity, the mirrorless devices would be very inefficient in terms of switching energy.

Intrinsic devices are all-optical, requiring no wires or electrodes for electrical feedback. The essential feedback is obtained by using an optical cavity, usually a Fabry–Perot etalon, and the intensity dependence of the intracavity absorption or refractive index. Often a nonlinearity associated with a resonance is utilized to reduce the required optical intensity; this may prevent room-temperature operation in some cases. The GaAs–GaAlAs device has not been operated above 120 K yet, but in other respects it has greater potential in terms of speed and switching energy. It is much smaller; only a 10- to 20-μm diameter of the 4.6-μm-thick sandwich was used. It is much faster (the cavity transit times are of the order of picoseconds) and requires less switching energy than the best integrated hybrid device to date; 40-nsec switching times were observed for a triangular-shaped input (≈5 nJ). The switch-on time was less than 1 nsec for a 0.6-nJ, 200-psec pulse spread over a diameter five times the cw beam diameter; this extrapolates to 25 pJ required for the actual active area. With further miniaturization, subpicojoule switching energy is anticipated. The small physical lengths of the cavity would enable tolerable wavelength stability, higher speeds, and even multimode operation to be achieved.

Both types of bistable device will, no doubt, find specialized applications. If size and electrical-power usage are of no concern, but broad-wavelength operating range is, then hybrid devices are appropriate. Mirrored, hybrid devices would require stringent wavelength stability. High-speed and high-packing-density operation at a single wavelength is likely to rely on intrinsic devices.

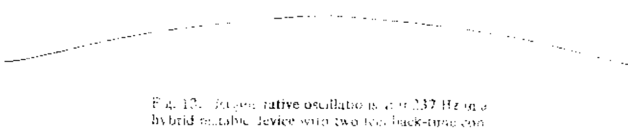

Fig. 13. [illegible] rative oscillations [illegible] 237 Hz in a hybrid bistable device with two feedback-time constants of [illegible] and 2/? [illegible] (Ref. 11).

DYNAMICS AND SPECTRA OF BISTABLE SYSTEMS

Bistable systems are intriguing dynamical systems. McCall has predicted and then observed regenerative pulsations: a cw input was converted into a train of light pulses (see Fig. 13).[11] Regions of positive slope $dI_T/dI_I > 0$ may not always be stable, as usually assumed in a steady-state analysis, and the device will then exhibit either premature switching or regenerative pulsations. McCall's hybrid experiment involved two different electrical time constants in the feedback loop. In an intrinsic system, the two times could have different physical origins; one might be electronic and the other thermal. Bonifacio *et al.* have discovered a different kind of regenerative pulsation in their bistability equations for operation on the upper branch with inputs just above the switching intensity.[28] Such pulsating devices constitute all-optical oscillators.

Several papers[11,29-34] have been devoted to the transient response of bistable optical devices. Bischofberger and Shen[30] have obtained impressive agreement between numerical simulations and experimental data for a nonlinear Fabry–Perot containing liquid crystals, CS_2, or nitrobenzene. They have studied the effects of cavity response time, medium response time, and input pulse length. They show that, even when the response is very fast, the transmission of a nonlinear Fabry–Perot still shows transient characteristics if the ratio of input pulse width (or characteristic time of input-intensity variation) to the cavity round-trip time is not sufficiently large (≈300 for a finesse of 13). This inertial sluggishness is an important consideration for hybrid devices having relatively long lengths (≈1 cm). But the above condition corresponds to 30-psec input pulse widths for the 5-μm GaAs device; shorter, lower-finesse devices might respond in times approaching 1 psec.

Bonifacio and Lugiato[28] predicted the lengthening of switching time when the increment to the input intensity is made smaller and smaller, holding the input intensity just below the switch-on value. This effect, referred to as critical slowing down, has been observed,[31] but it does not preclude rapid switching for a switching pulse of intensity sufficiently greater than the holding intensity. In fact, if the switch-on intensity is [illegible]% larger than the holding intensity, the switching time is only twice as long as the lifetime of the photons in the cavity.[33] The subnanosecond switch-on of the GaAs device illustrates [illegible]

Considerable [illegible]

has been devoted to the photon statistics and spectrum of the fluorescent and transmitted light in optical bistability of a Fabry–Perot or ring cavity containing two-level atoms.[35] The linewidth of the transmitted light becomes narrow as the field approaches the switch-on intensity from below. As the bistable device switches on, the spectrum splits discontinuously into a triplet (dynamical Stark shift). Such bistable systems are now regarded as ideal systems for studying first-order phase transitions in a system far from thermal equilibrium.

RELATED WORK

The present discussion has emphasized optical bistability in unexcited systems. Related effects have been seen[36] much earlier in lasing systems. Recently, Levin and Tang[36] observed optical bistability, multistability, and differential gain in an electro-optically tunable cw dye laser. Jain and Pratt[37] have proposed controlling a strong output signal with a weak input signal, using the strong dependence of second-harmonic generation on the phase-matching condition.

CONCLUSION

The field of optical bistability is just beginning. Development of tiny devices to manipulate lightwaves just as electronic devices manipulate electrons is under way. Although intrinsic optical devices are inherently more efficient and faster, hybrid optical bistable devices may find specific applications. The nonlinear properties of new optical materials need to be investigated to make intrinsic, efficient optical bistable devices. Optical bistability in truly integrated structures remains to be demonstrated.

REFERENCES

1. D. M. Bloom, L. F. Mollenauer, C. Lin, D. W. Taylor, and A. M. DelGaudio, Opt. Lett. 4, 297 (1979).
2. W. S. Boyle, Sci. Am. 237, 40 (1977).
3. A. Yariv, Sci. Am. 240, 64 (1979).
4. H. Seidel, U.S. Patent 3,610,731 (1969).
5. [illegible] Szöke, V. Daneu, J. Goldhar, and [illegible] Kurnit, Appl. Phys. Lett. 15, [illegible] (1969); A. Szöke, U.S. Patent [illegible] (1969).
6. [illegible] and [illegible] DeShazer, J. Opt. Soc. Am. 61, 650 (1971). J. W. Austin, Ph.D. dissertation, University of Southern California, Los Angeles, California, 1972.
7. E. Spiller, J. Opt. Soc. Am. 61, 669 (1971); J. Appl. Phys. 43, 1673 (1972).
8. S. L. McCall, Phys. Rev. A 9, 1515 (1974).
9. H. M. Gibbs, S. L. McCall, and T. N. C. Venkatesan, Phys. Rev. Lett. 36, 1135 (1976); S. L. McCall, H. M. Gibbs, G. G. Churchill, and T. N. C. Venkatesan, Bull. Am. Phys. Soc. 20, 636 (1975); S. L. McCall, H. M. Gibbs, and T. N. C. Venkatesan, J. Opt. Soc. Am. 65, 1184 (1975); U.S. Patents 4,012,699 (1975) and 4,121,167 (1976).
10. H. M. Gibbs, S. L. McCall, and T. N. C. Venkatesan, in *Coherence in Spectroscopy and Modern Physics*, F. T. Arecchi, R. Bonifacio, and M. O. Scully, eds. (Plenum, New York, 1978), p. 111.
11. S. L. McCall, Appl. Phys. Lett. 32, 284 (1978).
12. F. S. Felber and J. H. Marburger, Appl. Phys. Lett. 28, 731 (1976); J. H. Marburger and F. S. Felber, Phys. Rev. A 17, 335 (1978).
13. T. N. C. Venkatesan and S. L. McCall, Appl. Phys. Lett. 30, 282 (1977); T. N. C. Venkatesan, Ph.D. dissertation, City University of New York, New York 1977. Bistability was first seen in a solid-state system in ruby.
14. S. L. McCall and H. M. Gibbs, J. Opt. Soc. Am. 68, 1378 (1978); S. L. McCall, H. M. Gibbs, W. Greene, and A. Passner, unpublished.
15. H. M. Gibbs, S. L. McCall, T. N. C. Venkatesan, A. C. Gossard, A. Passner, and W. Wiegmann, in *Digest of 1979 IEEE/OSA Conference on Laser Engineering and Applications* (Institute of Electrical and Electronics Engineers, New York, 1979); in *Laser Spectroscopy IV*, H. Walther and K. W. Rothe, eds. (Springer-Verlag, Berlin, 1979); Appl. Phys. Lett., to be published (September 1, 1979).
16. C. V. Shank, R. L. Fork, R. F. Leheny, and J. Shah Phys. Rev. Lett. 42, 112 (1979).
17. H. M. Gibbs, T. N. C. Venkatesan, S. L. McCall, A. Passner, A. C. Gossard, and W. Wiegmann, Appl. Phys. Lett. 34, 511 (1979).
18. M. Okuda, M. Toyota, and K. Onaka, Opt. Commun. 19, 138 (1976); M. Okuda and K. Onaka, [illegible] J. Appl. Phys. 16, 303, [illegible] 17, 1105 [illegible] M. [illegible] K. Onaka, and T. [illegible] Appl. Phys. 17, 2123 [illegible]
19. [illegible] Semicond. 7, 825 [illegible]
20. P. W. Smith and [illegible] Appl. Phys. [illegible] 30, [illegible] For [illegible] bility using feedback from the reflected signal see P. W. Smith, E. H. Turner, and B. B. Mumford, Opt. Lett. 2, 55 (1978).
21. P. W. Smith, E. H. Turner, and P. J. Maloney, IEEE J. Quantum Electron. QE-14, 207 (1978).
22. M. Okaka and K. Takizawa, IEEE J. Quantum Electron. QE-15, 82 (1979).
23. E. Garmire, J. H. Marburger, and S. D. Allen, Appl. Phys. Lett. 32, 320 (1978).
24. A. Feldman, Opt. Lett. 4, 115 (1979); Appl. Phys. Lett. 33, 243 (1978).
25. P. S. Cross, R. V. Schmidt, R. L. Thornton, and P. W. Smith, IEEE J. Quantum Electron. QE-14, 577 (1978).
26. P. W. Smith, I. P. Kaminow, P. J. Maloney, and L. W. Stulz, Appl. Phys. Lett. 33, 24 (1978), 34, 62 (1979).
27. E. Garmire, S. D. Allen, J. Marburger, and C. M. Verber, Opt. Lett. 3, 69 (1978).
28. R. Bonifacio and L. A. Lugiato, Lett. Nuovo Cimento 21, 510 (1978); R. Bonifacio, M. Gronchi, and L. A. Lugiato, to be published.
29. M. Okuda and K. Onaka, Jpn. J. Appl. Phys. 17, 1105 (1978); M. Okuda, K. Onaka, and T. Sakai, Jpn. J. Appl. Phys. 17, 2123 (1978).
30. T. Bischofberger and Y. R. Shen, Appl. Phys. Lett. 32, 156 (1978); Opt. Lett. 4, 40 (1979); Phys. Rev. A 19, 1169 (1979).
31. E. Garmire, J. H. Marburger, S. D. Allen, and H. G. Winful, Appl. Phys. Lett. 34, 374 (1979).
32. R. Bonifacio and L. A. Lugiato, Opt. Commun. 19, 172 (1976).
33. R. Bonifacio and P. Meystre, Opt. Commun. 29, 131 (1979).
34. E. Abraham, R. K. Bullough, and S. S. Hassan, Opt. Commun. 29, 109 (1979).
35. R. Bonifacio and L. A. Lugiato, Phys. Rev. Lett. 40, 1023 (1978); L. M. Narducci, R. Gilmore, D. H. Feng, and G. S. Agarwal, Opt. Lett. 2, 88 (1978); G. S. Agarwal, L. M. Narducci, R. Gilmore, and D. H. Feng, Phys. Rev. A 18, 620 (1978); S. S. Hassan and D. F. Walls, J. Phys. A 11, L87 (1978).
36. V. N. Lisitsyn and V. P. Chebotaev, JETP Lett. 7, 1 (1978). A. P. Kozantsev, S. G. Rautian, and G. I. Surdutovich, Sov. Phys. JETP 27, 756 (1968); K. H. Levin and C. L. Tang, Appl. Phys. Lett. 34, 376 (1979); W. Neuhauser and P. E. Toschek, Opt. Commun. 28, 233 (1979); M. B. Spencer and W. E. Lamb, Jr., Phys. Rev. A 5, 884–893 (1972). A bistable laser was proposed by G. J. Lasher, Solid-State [illegible], 7, 707 (1964).
37. [illegible] Jain and [illegible] Pratt, Jr., Appl. Phys. Lett. 28, [illegible] (1976). See also L. M. [illegible] Pratt, Jr. Appl. Phys. Lett. 33, [illegible] (1978).